STUDIA UBB CHEMIA, LXXI, 1, 2026 (p. 101-119)
(RECOMMENDED CITATION)
DOI:10.24193/subbchem.2026.1.07

EFFECT OF FLUID VISCOSITY ON FLUIDIZATION HYDRODYNAMICS AN EXPERIMENTAL AND COMPARATIVE STUDY

Nassima KECHROUD[a*], Hamid TIGHZERT[a]

ABSTRACT. In this study, we conducted an experimental investigation of the fluidization behavior of spherical glass particles with diameters *dp*=2 mm and *dp*=4 mm, using Newtonian fluids (aqueous sugar solutions). The influence of fluid viscosity on key global hydrodynamic characteristics of fluidization was examined, including the minimum fluidization velocity, the terminal settling velocity of the particles, and bed expansion. Experiments were carried out in a cylindrical glass column with an inner diameter of *D*=20 mm and a height of *H*=1500 mm.

The minimum fluidization velocity and bed expansion were determined experimentally for different solid–liquid systems. The experimental results were compared with various correlations from the literature. It was found that the results are in good agreement with some of these correlations, particularly for bed porosity values below 0.6.

Keywords: *Fluidization; Newtonian fluid; hydrodynamic; effect of viscosity; expansion; minimum fluidization velocity; terminal settling velocity.*

INTRODUCTION

A fluidized bed is a system widely used in chemical engineering, where solid particles are suspended by an upward-flowing fluid (gas or liquid) resulting in a fluid-like behavior known as fluidization. This process occurs when the upward drag force exerted by the fluid counterbalances the weight of the particles, allowing them to remain suspended. Compared to fixed beds,

[a] *Department of Process Engineering, Faculty of Technology, Environmental Engineering Laboratory, Abderrahmane Mira University, Bejaia, Algeria*
* *Corresponding author: nassima.kechroud@univ-bejaia.dz*

©2026 STUDIA UBB CHEMIA. Published by Babeş-Bolyai University.
This work is licensed under a Creative Commons Attribution-NonCommercial-NoDerivatives 4.0 International License.

fluidized beds offer a significantly larger interfacial area between the solid particles and the fluid, enhancing phase interactions and transport processes [1-3]. This continuous movement promotes efficient heat and mass transfer, making fluidized beds highly suitable for a broad range of industrial applications. These include the chemical, petrochemical, pharmaceutical, metallurgical, biochemical, food processing, and waste treatment sectors, where fluidized beds are employed for operations such as particle coating, drying, combustion (fluidized-bed boilers), crystallization, and catalytic cracking [4]**.** Fluidized beds are also being examined for novel applications such as adsorption cooling and sustainable energy systems, demonstrating their ongoing industrial and environmental relevance [5].

The investigation of Newtonian fluidized bed hydrodynamics focuses on quantifying key parameters such as minimum fluidization velocity, pressure drop, and bed expansion. These are essential for the effective design, operation, and control of reactors. Over the past decades, considerable research has led to various empirical and semi-empirical correlations [2,6,7]. Despite the extensive development of this field, it remains of significant interest due to current industrial demands for improved energy efficiency, reduced costs, and stricter environmental regulations. In parallel, recent advances in computational fluid dynamics (CFD) and coupled CFD–Discrete Element Method (CFD-DEM) modeling have heightened the demand for high-quality experimental data to validate numerical predictions [8]. Accurate experimental characterization of Newtonian fluidized beds is therefore essential to improve existing correlations and to provide a reliable baseline for investigating more complex systems involving non-Newtonian fluids. In such systems, rheological effects strongly influence hydrodynamic behavior, making the prediction of key parameters, such as minimum fluidization velocity and bed expansion, considerably more challenging [4,9].

The main objective of the present study is to evaluate the influence of the rheological behavior of the fluid on key hydrodynamic characteristics, particularly the minimum fluidization velocity and bed expansion. The results obtained will be compared with established empirical correlations from the literature. Both minimum fluidization velocity and bed expansion are among the most influential parameters governing the dynamic behavior of fluidized beds. A comprehensive understanding of these factors is crucial in any effort to design predictive, adaptable, and efficient fluidized systems. This is precisely why the topic has long been, and continues to be, the subject of sustained research interest [10].

THEORETICAL BACKGROUND

Minimum Fluidization Velocity

The minimum fluidization point, marking the transition between a fixed and a fluidized bed, is typically characterized by the minimum fluidization velocity (U_{mf}) and the corresponding bed void fraction (ε_{mf}). Classical approaches, such as the Ergun correlation [1], estimate U_{mf} using fixed-bed equations while assuming specific values for ε_{mf} and the particle sphericity factor Φ. However, this method presents limitations, notably the need for parameters that are often difficult to determine experimentally. To address these issues, several researchers, including Riba et al. [11] and Coltters & Rivas [7], have developed simplified correlations.

Correlation of Riba et al. (1978)

Riba et al. [11] developed an empirical correlation to estimate the minimum fluidization velocity U_{mf} in fluidized beds. Their work aimed to improve the accuracy of predictions by taking into account a wide range of experimental conditions. The correlation relates U_{mf} to key physical properties such as particle diameter (d_p)**,** particle and fluid densities $(\rho_s; \rho_f)$, and fluid viscosity (μ):

$$Re_{mf} = 0.0154 \times Ga^{0.66} \times Mn^{0.7} \quad (1)$$

Where Re_{mf}, *Ga* and *Mv* are defined as:

$$Re_{mf} = \frac{\rho_f U_{mf} d_p}{\mu} ; Ga = \frac{d_p^3 \rho_f g}{\mu^2} ; Mn = \frac{\rho_s - \rho_f}{\rho_f} \quad (2)$$

Correlation of Coltters and Rivas (2004)

Coltters and Rivas (7] compiled 189 experimental measurements from the literature, covering approximately 89 different materials (sand, coal, polymers, glass, etc.) fluidized by a gas phase. For each material, the authors established a correlation that differs significantly from those commonly found in the literature. To predict the minimum fluidization velocity for glass particles with an average diameter between 569 µm and 3000 µm, the authors proposed the following correlation:

$$U_{mf} = (2.4624.10^{-3}) X^{(0.46942 \mp 0.01190)} \quad (3)$$

With:

$$X = \frac{d_p^2 (\rho_s - \rho_f) g}{\mu} . \left(\frac{\rho_s}{\rho_f}\right)^{1.23} \quad (4)$$

Porosity and Bed Expansion

Solid–liquid fluidized bed systems are characterized by a progressive and uniform expansion of the bed with increasing liquid velocity. This expansion is typically described in terms of bed porosity (or void fraction) *e*. The expansion process occurs between the minimum fluidization velocity and the terminal settling velocity of the particles, during which the bed height increases as a function of liquid velocity.

A widely used approach to determine the void fraction is based on measuring the expanded bed height, *H*.

$$\varepsilon = 1 - \frac{m_p}{HS\rho_S} \tag{5}$$

Where $\mathrm{m_p}$ is the mass of solid particles (kg), S is the cross-sectional area of the column (m²), and ρ_s is the density of solid particles (kg/m³).

Several correlations have been developed to describe the expansion of solid–liquid fluidized beds. Some of these take into account the terminal settling velocity of the particles (U_t), while others are based on different variables.

Correlations Independent of U_t

Correlation of Wen & Yu (1966)

Among the researchers who have contributed to improving the modeling of liquid fluidized bed expansion, Wen and Yu [2] are frequently cited. Based on a force balance during bed expansion, these authors proposed the following theoretical model:

$$\varepsilon^{-4,7} = \frac{Ga.Mn}{18\,Re + 2{,}7Re^{1{,}687}} \tag{6}$$

Correlation of Miura et al. (2000)

Miura et al. [9] examined the expansion characteristics of a fluidized bed composed of 3 mm glass beads using water and aqueous glycerol solutions as the fluidizing media. For a terminal Reynolds number ranging from 8.14 to 3947, the authors proposed the following correlation:

$$\varepsilon = \left(\left(18\frac{\mu U}{d_p^2} + 3\sqrt{\frac{\mu\rho_f U^3}{d_p^3}} + 0.3\frac{\rho_f U^2}{d_p} \right) \frac{1}{(\rho_s - \rho_f)g} \right)^{0{,}208} \tag{7}$$

Correlations Dependent of U_t

Richardson and Zaki [6] described bed expansion using a correlation between the bed porosity ε and the ratio of the superficial liquid velocity U to the terminal settling velocity U_t of an individual particle, as given by the following expression :

$$\frac{U}{U_t} = \varepsilon^Z \tag{8}$$

Where *Z* is the fluidization index (also known as the Richardson–Zaki exponent), which depends on the particle Reynolds number during settling (Re_t) and the particle-to-column diameter ratio ($\frac{d_p}{D}$). The value of Z is determined using the empirical correlations listed in Table 1.

Table 1: Empirical values of *Z* and applicable Re_t ranges

Correlation	Reynolds number
$z = 4.65 + 19.5\left(\frac{dp}{D}\right)$	$Re_t < 0{,}2$
$z = \left(4.45 + 18\frac{dp}{D}\right) Re_t^{-0.03}$	$0.2 < Re_t < 1$
$z = \left(4.45 + 18\frac{dp}{D}\right) Re_t^{-0,1}$	$1 < Re_t < 200$
$z = 4.45\ Re_t^{-0.1}$	$200 < Re_t < 500$
$z = 2.4$	$500 < Re_t$

Among the different formulas proposed to calculate the terminal Reynolds number (Re_t) or the terminal settling velocity (U_t), those developed by Lali et al. [12] are especially noteworthy. To study how the walls of a container affect the settling speed of particles in water–glycerol mixtures, the authors carried out experiments using nine vertical columns with diameters ranging from 0.9 to 20 cm. They used spherical particles made of glass and steel, with densities of 2500 kg/m³ and 1180 kg/m³, respectively. The particle diameters ranged from 1.2 to 25 mm for glass and from 0.8 to 20 mm for steel. This gave particle-to-column diameter ratios ($\frac{d_p}{D}$) between 0.05 and 0.78.

The authors proposed formulas that cover a wide range of infinite Reynolds numbers (Re_∞), which are listed in Table 2. These correlations allow for the estimation of $Re_¥$ (or $U_¥$) based solely on the Archimedes number.

Table 2: Correlations of Lali et al. (1989)

Correlations	Values of Re_∞	Values of *Ar*
$Re_\infty = \frac{Ar}{18}$	$Re_\infty < 1$	$Ar < 1.8$
$Re_\infty = \left(\frac{Ar}{18}\right)^{0,8}$	$1 < Re_\infty < 56$	$1.8 < Ar < 2600$
$Re_\infty = 0.45 \acute{} Ar^{0,61}$	$56 < Re_\infty < 1000$	$2.6 \acute{} 10^3 < Ar < 3.3 \acute{} 10^5$
$Re_\infty = 1.732 \acute{} Ar^{0,50}$	$Re_¥ > 10^3$	$Ar > 3.3 \acute{} 10^5$

Zigrang and Sylvester [13], building upon the work of Barnea & Mizrahi [14] and Barnea & Mednick [15] on solid–fluid suspensions, proposed an explicit equation for the particle settling velocity in solid–fluid systems. Their equation is expressed in terms of $Re_¥$ and the Archimedes number Ar:

$$Re_t = 1.8329 \acute{} Ar^{1/2} + 29.025 - \left(106.4 \acute{} Ar^{1/2} + 842.45\right)^{1/2} \quad (9)$$

RESULTS AND DISCUSSION

The different systems studied, as well as the ranges of velocity and porosity explored, are summarized in Tables 3 and 4.

It should be noted that the dimensionless Archimedes number (Ar), particle Reynolds number (Rep), Galileo number (Ga), and density ratio (Mv) presented in these tables are calculated using the mean diameter and density of the spherical glass particles studied:

$$Ar = \frac{dp^3 \rho_f (\rho_s - \rho_f) g}{\mu^2}; \quad Ga = \frac{dp^3 \rho_f^2}{\mu^2}; \quad Re_p = \frac{\rho_f U dp}{\mu}; \quad Mn = \frac{(\rho_s - \rho_f)}{\rho_f}$$

Table 3: Experimental study parameters for particles with a diameter of d_p = 2mm and a density of r_p=2554 kg/m^3

m (Pa.s)	r_f (kg/m^3)	U(m/s)	Re	e	Ar	Ga	Mn
0.001	1000	0.014-0.106	28 - 212	0.40-0.76	122000	78480	1.55
0.002	1040	0.0017–0.0427	2 - 46	0.40- 0.58	32833	22554	1.46
0.006	1060	0.014-0.091	29 -196	0.40-0.69	3570	2533	1.41

Table 4: Experimental study parameters for particles with a diameter of d_p = 4mm and a density of r_p=2564 kg/m^3

m(Pa.s)	r_f (kg/m^3)	U(m/s)	Re	e	Ar	Ga	Mn
0.001	1000	0.098-0.024	94-393	0.40-0.64	982000	627840	1.56
0.002	1040	0.091–0.014	29-196	0.40-0.69	264401	180431	1.46
0.006	1060	0.003-0.052	2- 8	0.40-0.59	28754	20266	1.41

Determination of the Minimum Fluidization Velocity

To experimentally determine the minimum fluidization velocity for a given fluid–solid system, we adopted the standard method commonly used [2,16], which involves analyzing the ΔP–U plot. This method requires plotting the pressure drop (ΔP) as a function of the superficial velocity (U) in the fixed bed region and identifying its intersection with the line representing the constant pressure drop in the fluidized bed. For the six (sphere–fluid) systems studied, we plotted the variations in pressure drop as a function of the fluid superficial velocity and graphically determined the minimum fluidization velocity. Measurements were carried out by progressively increasing the flow rate up to the maximum fluidization limit, followed by a gradual decrease in flow rate. As shown in Figure 1, the minimum fluidization velocity corresponds to the point marking the transition between the fixed and fluidized states.

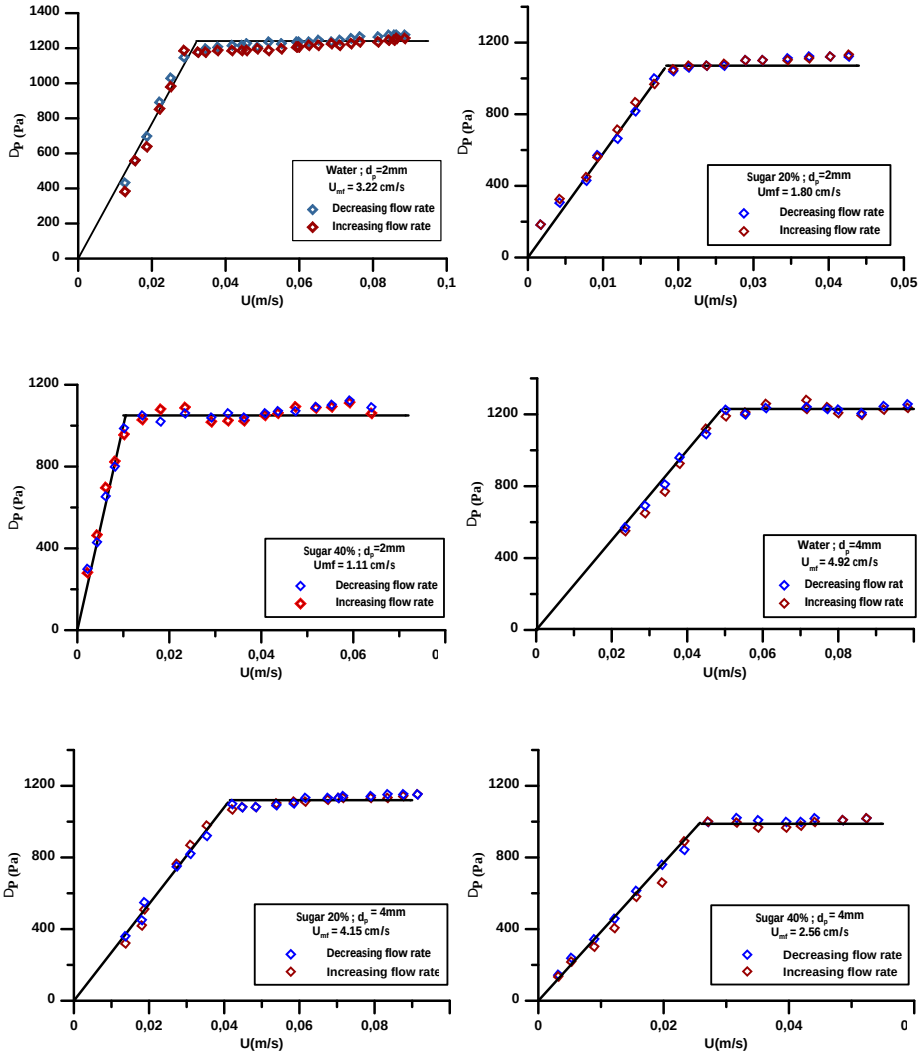

Figure 1: Pressure drop as a function of the fluid superficial velocity

The results are summarized in Table 5.

Table 5: Experimental values of the minimum fluidization velocity for all systems studied

d_p (mm)	μ (Pa.s)	ρ_f (kg/m^3)	U_{mf} (cm/s)
2	0.001	1000	3.22
	0.002	1040	1.80
	0.006	1060	1.11
4	0,001	1000	4.92
	0,002	1040	4.15
	0,006	1060	2.56

The results show that as the viscosity of the solution increases, the minimum fluidization velocity (U_{mf}) decreases. This decrease in U_{mf} can be explained by the fact that viscous forces become significant enough to support the apparent weight of the particles, making it possible to suspend them at lower flow rates.

Comparaison to the Litterature

Because fluidized bed flows involve complex phenomena, a full theoretical explanation is not provided here. Instead, we focus on using mathematical expressions that best describe the observed hydrodynamic behavior. To this end, the experimental results obtained in the present study are compared with those predicted by correlations from the literature.

We compared our experimental results with the minimum fluidization velocities predicted by two empirical correlations of Riba et al. [11] and Coltters and Rivas [7]. These predictions were compared to our experimental data by calculating the relative differences between the U_{mf} values given by the correlations and those measured in the experiments. Table 6 shows the average relative deviation, calculated using the following equation [10]:

$$E\,(\%) = \frac{\left|\left(U_{mf}\right)_{exp} - \left(U_{mf}\right)_{cal}\right|}{\left(\frac{\left(U_{mf}\right)_{exp} + \left(U_{mf}\right)_{cal}}{2}\right)} \times 100 \qquad (10)$$

Table 6: Relative deviations between the experimental minimum fluidization velocity and the values calculated using literature correlations for Newtonian fluidization

d_p (mm)	μ (Pa.s)	$U_{mf\ exp}$ (cm/s)	Riba et al. (1978)			Coltters and Rivas (2004)		
			Re_{mf}	U_{mf} (cm/s)	E%	Re_{mf}	U_{mf} (cm/s)	E%
2	0.001	3.22	35.59	1.78	57.63	58.40	2.92	9.78
	0.002	1.80	14.99	1.44	22.15	21.17	2.03	12.27
	0.006	1.11	3.45	0.98	11.78	4.22	1.19	8.18
4	0.001	4.92	141.02	3.52	33.02	225.33	5.63	13.51
	0.002	4.18	59.12	2.84	37.40	81.67	3.93	5.53
	0.006	2.56	13.67	1.93	28.14	16.27	2.30	10.59

The results obtained show that the accuracy of the correlation by Coltters and Rivas [7] is significantly higher than that of Riba et al. [11], as the observed relative deviations do not exceed 14%.

Bed Expansion and Porosity

Figure 2 shows the evolution of porosity as a function of fluid flow velocity. The porosity values obtained during increasing and decreasing flow rates exhibit minimal discrepancy, with the relative deviation across all systems investigated remaining below 0.1%. Up to the minimum fluidization velocity, porosity remains nearly constant. Beyond this threshold, a gradual increase in porosity is observed with increasing velocity, indicating a progressive expansion of the particle bed.

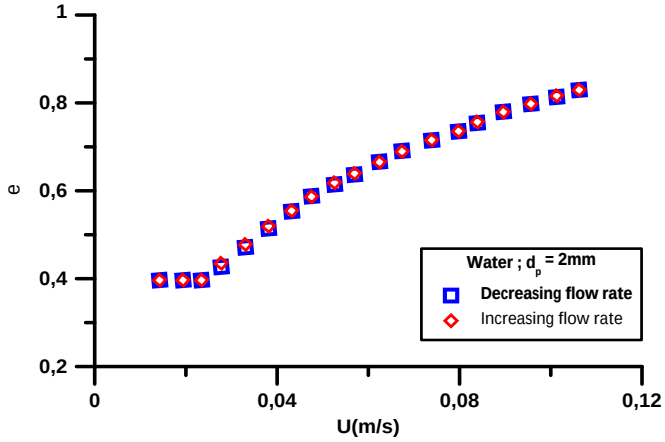

Figure 2: Exemple of the variation of bed porosity as a function of fluid velocity

Effect of Fluid Viscosity on Bed Expansion

Figure 3 presents the variation of porosity as a function of fluid velocity for the three Newtonian fluids investigated: water, and aqueous sugar solutions at 20 wt% and 40 wt%.

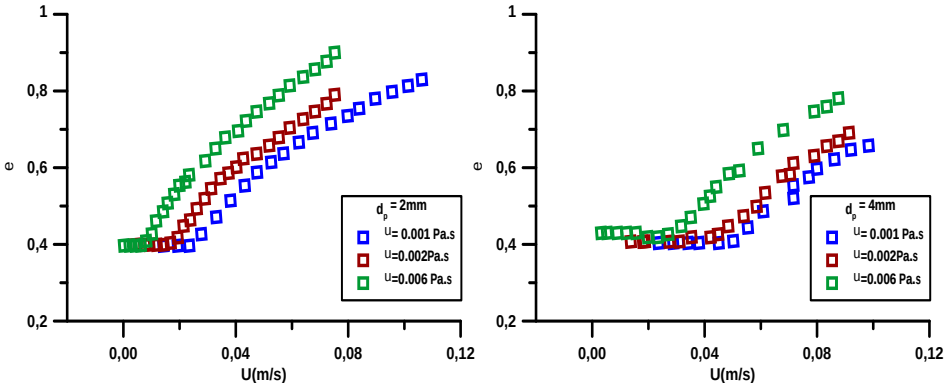

Figure 3: The effect of dynamic viscosity on the porosity evolution of the fluidized bed

It is observed that, for a given flow velocity, the porosity increases with the viscosity of the fluid. Similar observations were reported by Miura et al. [9] in their study on aqueous glycerol solutions (60%, 75%, and 83% by mass).

Correlations involving Ut

A large number of correlations reported in the literature involve the terminal settling velocity U_t. In general, the expansion behavior of fluidized beds is commonly described by the Richardson and Zaki [6] correlation:

$$\frac{U}{U_t} = \varepsilon^Z \qquad (11)$$

Richardson and Zaki [6] demonstrated that the parameter Z, often referred to as the fluidization index, depends solely on wall effects in both laminar and turbulent regimes. In the intermediate regime, however, Z is influenced by both wall effects and the settling Reynolds number Re_t, which is based on the settling velocity of an isolated particle.

To determine the expansion characteristics as predicted by the Richardson and Zaki [6] model, we used the experimental values of U_t obtained in the present study (see Figure 4). The parameter Z was calculated using the correlation proposed by Garside and Al-Dibouni [17].

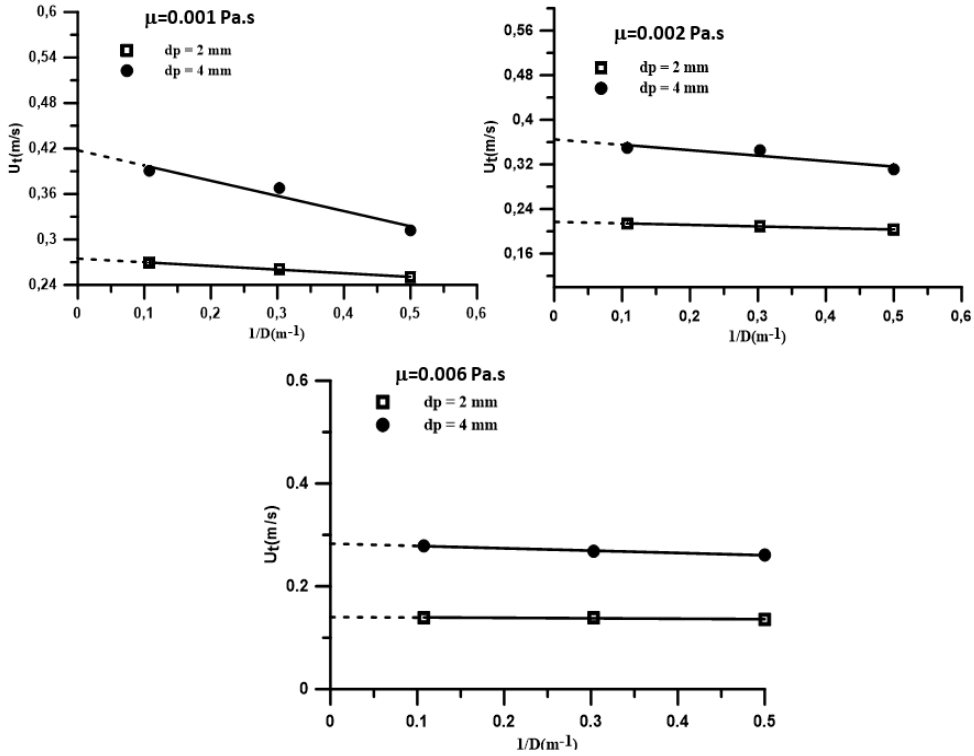

Figure 4: Variation of particle settling velocity with test column diameter

Based on the obtained graphs, the variation appears to be quasi-linear. Consequently, it is relatively easy to determine, by extrapolation, the particle settling velocity in the absence of wall effects U_∞ (corresponding to $D \rightarrow \infty$). The values thus obtained are presented in the following table.

Table 7: Experimental Values of U_∞

r_f (kg/m^3)	m (Pa.s)	d_p = 2 mm		d_p = 4 mm	
		U_∞ (m/s)	Rep_∞	U_∞ (cm/s)	Rep_∞
1000	0.001	0.27	550	0.43	1672
1040	0.002	0.22	232	0.36	783
1060	0.006	0.14	50	0.28	205

Our experimental results were compared with the predictions from the correlations proposed by Lali et al. [12] and Zigrang & Sylvester [13]. The results of this comparison are summarized in the table below.

Table 8: U_∞ Values calculated from selected correlations and comparison with experimental Data

d_p = 2 mm							
ρ_f (kg/m^3)	μ (Pa.s)	U_∞ (m/s)	Rep_∞	Zigrang & Sylvester (1981)		Lali et al. (1989)	
				Rep_∞	E(%)	Rep_∞	E(%)
1000	0.001	0.27	550	474	15	570	4
1040	0.002	0.22	232	219	6	256	10
1060	0.006	0.14	50	54	7	66	28
d_p = 4 mm							
1000	1	0.43	1672	1519	10	2034	20
1040	1,94	0.36	783	736	6	914	15
1060	5,9	0.28	205	202	1	236	14

In light of these results, it can be observed that the Rep_∞ values predicted by the correlation of Zigrang and Sylvester [13] are in better agreement with the experimental values obtained in the present study.

To evaluate the expansion behavior as predicted by the Richardson and Zaki [6] correlation, the experimental terminal velocities (U_t) measured in this study were used. The parameter Z was calculated using the correlation proposed by Garside and Al-Dibouni [17], and the corresponding values are presented in Table 9.

Table 9: Experimental values of U_t and fluidization indices

μ (Pa.s)	d_p = 2 mm			d_p = 4 mm		
	U_t (m/s)	Re_t	Z	U_t (m/s)	Re_t	Z
0.001	0.27	550	2.81	0.43	1672	2.76
0.002	0.22	232	2.90	0.36	783	2.79
0.006	0.14	50	3.27	0.28	205	2.92

Comparison of Fluidized Bed Expansion with Literature Correlations

Figure 5 shows the variation of bed porosity as a function of superficial fluid velocity for the different systems studied, along with predictions obtained from the correlations of Miura et al. [9], Wen and Yu [2], and Richardson and Zaki [6].

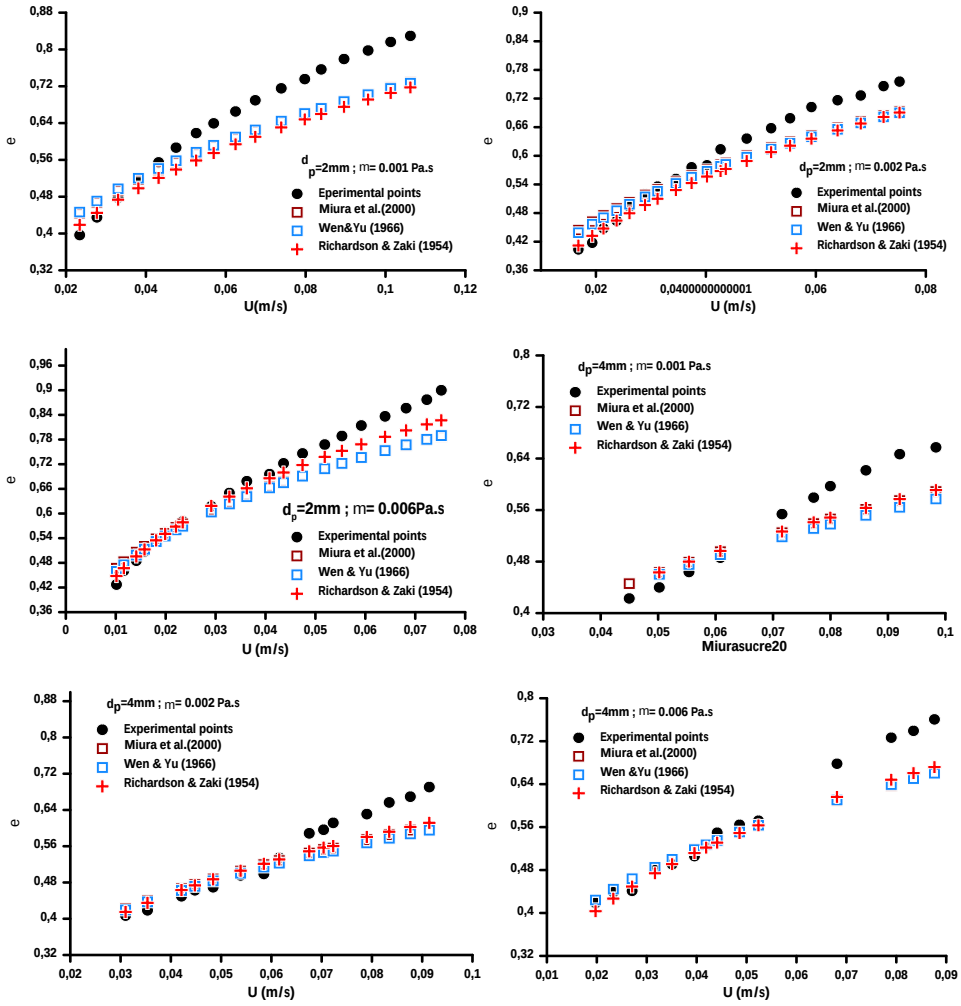

Figure 5: Comparison of bed expansion data with correlations from the literature

To identify the range of porosity in which the predictions can be considered highly satisfactory, the Root Mean Square Error (RMSE) was calculated between the experimental values and those predicted by the selected correlations for each solid–fluid system. The RMSE is computed using the following equation [18]:

$$RMSE = \left(\sum_{i=1}^{n}\left(\frac{\left(\varepsilon_{iexp}-\varepsilon_{ical}\right)^2}{n}\right)\right)^{1/2} \quad (11)$$

where ε_{iexp} denotes the experimental value, ε_{ical} the simulated value, and n the total number of values.

The results, summarized in Tables 10 and 11, show that the RMSE values are highly satisfactory for porosity values below 0.6. However, from ε = 0.6 onwards, the deviation between the calculated and experimental porosity values becomes more significant across all the systems studied.

Table 10: Root mean square errors by porosity range between experimental bed porosity values and those calculated using the selected correlations (for d_p = 2 mm)

RMSE						
m **(Pa.s)**	**0.001**		**0.002**		**0.006**	
Bed Porosity	$\varepsilon < 0.6$	$\varepsilon > 0.6$	$\varepsilon < 0.6$	$\varepsilon > 0.6$	$\varepsilon < 0.6$	$\varepsilon > 0.6$
Miura et al. (2000)	0.03	0.08	0.02	0.05	0.02	0.07
Wen & Yu (1966)	0.03	0.08	0.02	0.05	0.01	0.07
Richardson &Zaki (1954)	0.03	0.09	0.02	0.06	0.01	0.04

Table 11: Root mean square errors by porosity range between experimental bed porosity values and those calculated using the selected correlations (for d_p = 4 mm)

RMSE						
m **(Pa.s)**	**0.001**		**0.002**		**0.006**	
Bed Porosity	$\varepsilon < 0.6$	$\varepsilon > 0.6$	$\varepsilon < 0.6$	$\varepsilon > 0.6$	$\varepsilon < 0.6$	$\varepsilon > 0.6$
Miura et al. (2000)	0.03	0.07	0.02	0.07	0.01	0.09
Wen & Yu (1966)	0.03	0.08	0.02	0.08	0.02	0.08
Richardson &Zaki (1954)	0.03	0.06	0.02	0.06	0.01	0.07

CONCLUSION

In this study, experiments were conducted on a liquid–solid fluidized bed using a glass column with an internal diameter of 2 mm and a height of 150 mm. Glass particles with diameters of 2 mm and 4 mm were fluidized using tap water and aqueous sugar solutions at concentrations of 20 wt% and 40 wt%, maintained at 20 ± 1 °C. The minimum fluidization velocity (U_{mf}) and bed porosity were determined under various operating conditions. Results indicate that U_{mf} decreases with increasing fluid viscosity. The experimental U_{mf} values showed the best agreement with the correlation proposed by Coltters and Rivas [7], with mean relative deviations below 15%. For a given superficial velocity, bed porosity increased with fluid viscosity. Although the Richardson and Zaki [6] correlation, which requires knowledge of the particle terminal settling velocity, provided accurate porosity predictions for values below 0.6, this study demonstrates that such measurements are not essential. In fact, the correlations proposed by Wen and Yu [2] and Miura et al. [9], which do not require settling velocity data, yielded predictions in close agreement with experimental values. These findings confirm that accurate estimation of bed expansion can be achieved without prior knowledge of terminal settling velocity, thereby simplifying the hydrodynamic modeling of liquid–solid fluidized systems.

Future work could extend this study to a broader range of particle and column sizes, as well as to non-Newtonian fluids, thereby broadening the scope of the present results and generating a valuable dataset for establishing correlations and supporting simulation and modeling studies.

EXPERIMENTAL FLUIDIZED BED SETUP

The fluidization of spherical particles using a Newtonian aqueous sugar solution was studied using the experimental setup shown in figure 6-a). The setup consists of a cylindrical glass column (1) with an inner diameter of 2 cm and a height of 150 cm. Different particle beds were placed inside the column, supported by a liquid distributor (2) made of a fine-mesh grid. Since liquid flow can be uneven (following preferential paths), a flow-stabilizing section is positioned before the fluidization column. This homogenization section (3) has the same diameter as the column and a height of 12 cm.

The liquid is circulated from a supply tank (4) using a centrifugal pump (5) with a flow rate of 35 L/min. A thermostat (6), placed directly in the liquid, is used to monitor the temperature. The pipe feeding the column includes a bypass valve (7)

that redirects excess liquid back to the tank if necessary. Two flowmeters (8), installed in parallel after the pump, measure the flow rate. After passing through the column, the liquid flows back to the tank via a conical outlet (collector) (9). The conical shape helps minimize air bubble formation during discharge. The liquid returns to the tank through a small-diameter tube to ensure a steady flow. At the top, a fine-mesh grid (10) separates the return path from the main column. The experimental setup also includes a manometer (11) for measuring pressure within the fluidized bed. A metal ruler (12), marked with a scale, is used to measure the bed expansion.

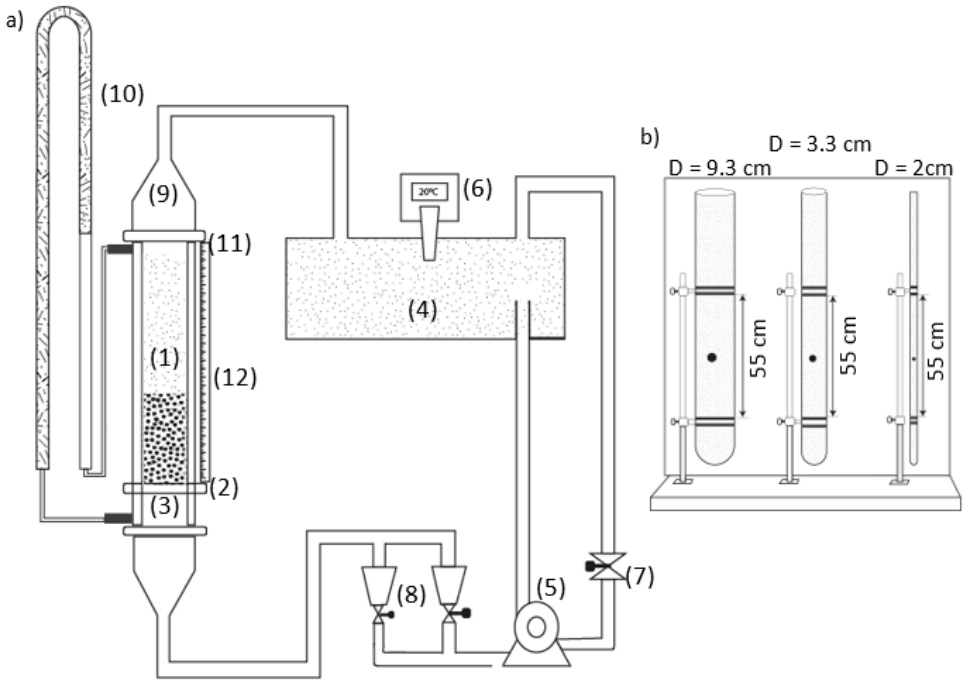

Figure 6: Experimental setup

(1) Test colmun; (2): Liquid distributor; (3): Homogenisation section; (4): Tank; (5): Pump; (6): Themostat; (7): Bypass; (8): Flowmeters; (9): Collector; (10): Manometric rule; (11): Fine-mesh grid; (12): Metal ruler.

The solid particles used in this study are glass spheres, with their physical properties listed in table 12. The fluids used consist of water and Newtonian aqueous sugar solutions containing 20% and 40% sugar by mass. These solutions were prepared by dissolving the appropriate amount of commercial sugar in water under constant stirring until complete dissolution

was achieved. The prepared solutions were then left to stand for 24 hours to allow any entrapped air to escape. The viscosities of the sugar solutions were measured using a HAAKE rheometer equipped with a Couette geometry (two concentric rotating cylinders. Since viscosity is highly sensitive to temperature, the measurement temperature was carefully controlled and is reported to ensure the reliability of the results. The values presented in Table 12 represent the average of three independent measurements for each solution.

Table 12: Fluid and solid properties

Solid properties			
***dp* (mm)**	2	4	
ρ_s (kg/m^3)	2554	2564	
Fluid properties			
Fluid	**Water**	**Sugar solution at 20% w/w**	**Sugar solution at 40% w/w**
ρ_f (kg/m^3)	1000	1040	1060
μ (Pa.s)	0.001	0.002	0.006

To determine the terminal settling velocity of the studied glass particles, experiments were conducted using three vertical columns with internal diameters of 2.0 cm, 3.3 cm, and 9.3 cm (see Figure 6-b)). After thorough cleaning, each column was filled with the test liquid and allowed to stand for approximately 12 hours to eliminate any trapped air bubbles and to ensure uniform fluid conditions. Simultaneously, the glass particles were immersed in the same liquid for about 6 hours to achieve complete wetting and thermal equilibrium. During the measurements, a single particle was released as close as possible to the central axis of the column. The descent time (*t*) was recorded between two fixed positions: 10 cm below the liquid surface and 10 cm above the bottom of the column, in order to minimize entrance and wall effects. The effective falling distance was *L*=55cm. Each test was performed in random order, and multiple repetitions were carried out to minimize measurement uncertainty. For each set of conditions, the reported terminal settling velocity corresponds to the average of at least 20 individual measurements and was calculated using the equation:

$$U_t = \frac{L}{t} \tag{12}$$

ACKNOWLEDGMENTS

The authors are grateful for the financial support of the Ministry of Higher Studies and Scientific Research of Algeria.

REFERENCES

1. S. Ergun**;** *Chemical Engineering Progress,* **1952**, *48*, 89–94.
2. C. Y. Wen; Y. H. Yu; *Chemical Engineering Progress Symposium Series*, **1966**, *62*, 100–111.
3. J. Balag; D. A. T. Franco; V. G. Miral; V. Reyes; L. J. Tongco; E. C. R. Lopez; *Engineering Proceedings*, **2023**, *56*, 62.
4. A. H. Darweesh; M. M. Weis; *Advanced Mechanical and Materials Engineering,* **2024**, *41*, 39–46.
5. Ł. Lasek; A. Zylka; J. Krzywański; D. Skrobek; K. Sztekler; W. Nowak; *Energies*, **2023**, *16*, 7311.
6. J. F. Richardson; W. N. Zaki; *Transactions of the Institution of Chemical Engineers*, **1954**, *32*, 35–53.
7. R. Coltters; A. L. Rivas; *Powder Technology*, **2004**, *147*, 34–48.
8. M. J. A. de Munck; E. A. J. F. Peters; J. A. M. Kuipers; *Industrial & Engineering Chemistry Research,* **2023**, *62*, 16687–16701.
9. H. Miura; T. Takahashi; J. Ichikawa; Y. Kawase; *Powder Technology,* **2001**, *117*, 239–246.
10. A. Kaur; A. Sobti; R. K. Wanchoo; *Industrial & Engineering Chemistry Research*, **2023**, *62*, 18704–18719.
11. J. P. Riba; R. Routié; J. P. Couderc; *Canadian Journal of Chemical Engineering,* **1978**, *56*, 26–30.
12. A. M. Lali; A. S. Khare; J. B. Joshi; K. D. P. Nigam; *Powder Technology*, **1989**, *57*, 39–50.
13. D. J. Zigrang; N. D. Sylvester; *AIChE Journal,* **1981**, *27*, 1043–1044.
14. E. Barnea; J. Mizrahi; *Chemical Engineering Journal*, **1973**, *5*, 171–189.
15. E. Barnea; R. L. Mednick; *Chemical Engineering Journal,* **1978**, *15*, 215–227.
16. L. D. Boset; Z. A. Debele; A. W. Koroso; *Journal of Heat and Mass Transfer Research*, **2025**, in press.
17. J. Garside; M. R. Al-Dibouni; *Industrial & Engineering Chemistry Process Design and Development,* **1977**, *16*, 206–214.
18. S. P. Neill; M. R. Hashemi; Fundamentals of Ocean Renewable Energy, **2018**.